Hindawi
Journal of Nanomaterials
Volume 2020, Article ID 4072351, 9 pages
https://doi.org/10.1155/2020/4072351

Research Article

Influence of Seed Layer Surface Position on Morphology and Photocatalysis Efficiency of ZnO Nanorods and Nanoflowers

Fouzia Bourfaa,[1] **Abderhamane Boutelala**,[1] **Mohamed Salah Aida**,[1,2] **Nadir Attaf**,[1] **and Yusuf Selim Ocak**[3]

[1]*Laboratory of Thin Films and Interfaces, Faculty of Science, University of Brothers Mentouri Constantine 1, Algeria*
[2]*Department of Physics, King Abdul-Aziz University, Jeddah, Saudi Arabia*
[3]*Department of Science, Faculty of Education, Dicle University, 21280 Diyarbakir, Turkey*

Correspondence should be addressed to Fouzia Bourfaa; fouzia_bourfaa@yahoo.fr

Received 11 September 2019; Revised 14 November 2019; Accepted 28 November 2019; Published 4 January 2020

Academic Editor: Kishore Sridharan

ZnO nanorods and nanoflowers were synthesized by a hydrothermal method via different surface substrate positions at 120°C for 3 h as a growth time. The influence of seed layer surface position on the growth of ZnO nanostructures was observed by the variation of ZnO morphologies from nanorods to nanoflowers. Both analyses XRD and EDS proved the pure wurtzite phase with high crystallinity quality and preferential growth along the *c*-axis. As displayed from the scanning of surface morphology through SEM, a large amount of ZnO nanorods and nanoflowers were deposited on the full substrate surface. Diverse ZnO photocatalysts were used to study the photodegradation of Methylene Blue (MB) dye by UV light. The organic dye MB was decolorized by the most efficient photocatalyst among the ZnO-tested nanostructures. The results showed an improvement of the degradability of this dye from 54% to 81% for ZnO nanoflowers compared to nanorods. Thus, ZnO nanoflowers are the best photocatalyst which have the high efficiency photodegradation and the large rate constant.

1. Introduction

One-dimensional (1D) ZnO nanostructured semiconductor photocatalysts have received in recent years an enormous attention because of their wide-spread applications in environmental treatment [1]. These ZnO photocatalysts have a high efficiency for the degradation of toxic organic pollutants. Zinc oxide as a II-IV semiconductor with a wide band gap (3.37 eV) and a large exciton binding energy (60 meV) is considered as a promising material for purification and disinfection of water and air. ZnO as a photocatalyst was consumed extensively for the photodegradation of organic dyes [2–4]. Nanostructured ZnO has been synthesized in various morphologies like nanowires, nanorods, nanobelts, nanoneedles, and nanoflowers which have enticed a significant interest owing to their promising applications such as gas sensing [5], light-emitting diodes (LEDs) [6], antibacterial agent [7], solar cells [8, 9], and photocatalysis [10, 11].

The photocatalysis activity was effectuated through two mechanisms: the oxidation and reduction reaction in the presence of photocatalyst. Generally, in this process, the photogenerated holes which have a high oxidation power in the valence band (VB) and photogenerated electrons in the conduction band (CB) which have sufficient reduction power are necessary for efficient photocatalytic reactions. The fundamental processes of the photocatalysis activity of Methylene Blue (MB) dye can be understood as follows. The first stage involves adsorption of MB onto the ZnO nanostructures. Irradiation with UV light or sunlight leads to the generation of electron– hole (e^-–h^+) pairs in ZnO. The electrons (e^-) in the conduction band of ZnO react with oxygen molecules adsorbed on ZnO to form superoxide anion radicals ($^{\cdot}O_2^-$). The holes (h^+) generated in the valence band of ZnO interact with surface hydroxy groups to produce highly reactive hydroxyl ($^{\cdot}OH$) radicals. The photogenerated holes can perform to the production of $^{\cdot}OH$ radicals through the

dissociation of water. The superoxide radicals ($^{\cdot}O_2^-$) and highly reactive hydroxyl radicals ($^{\cdot}OH$) react with MB adsorbed on ZnO nanostructures and lead to the degradation of MB.

Newly, several approaches were developed for synthesis of ZnO nanomaterials as well as vapor-phase transport [12], chemical vapor deposition [13], magnetron sputtering [14], pulsed laser deposition [15], wet chemical method [16], and hydrothermal processing [10, 17, 18]. The hydrothermal method is one of the vastest ways for growth of ZnO nanostructures compared with other methods. This process is a very promising method for fabricating ideal nanostructures with special and different morphologies. Hydrothermal synthesis has gained numerous interest from scientists in general and chemists in particular for its operational simplicity, low cost, low temperature, high yield, and scalable process.

ZnO nanostructures have also tested different pollutants other than the Methylene Blue by various researches. Fan et al. [10] fabricated ZnO nanoflowers on Si substrate by the hydrothermal method at 70 and 80°C for 70 min, and the photocatalysis activity of Rhodamine dye with a concentration of 5 mg/l by ZnO nanoflowers/Si was investigated. The photodegradation efficiency after 3 h of irradiation time was found 42% and 52% for ZnO nanoflowers at 70 and 80°C, respectively.

Kuriakose et al. [16] synthesized flower-like ZnO nanostructures at 60°C for 3 h with different concentrations of zinc acetate 0.02, 0.05, and 0.1 M for preparing three samples S1, S2, and S3. The photodegradation of Methylene Blue by these photocatalysts was studied with a concentration of 22.4 μM while the efficiency of each sample was achieved 97.8%, 99.6%, and 66.8% for S1, S2, and S3, respectively, after 60 min of sunlight exposure.

Habba et al. [18] studied the photocatalytic activity of the ZnO NWs of Methylene Blue (MB), Methyl Orange (MO), and Azorubine (acid red 14—AR14) with concentration of 10 μM for each dye. The undoped ZnO NWs and Fe-doped NWs were synthesized at 95°C and for 4 h by the hydrothermal process. The degradation rate of ZnO NWs and ZnO:1% Fe NWs, respectively, was found 49%-69% for MO, 86%-95% for MB, and 93%-98% for AR14 after 3 h of illumination.

Furthermore, an X-ray diffraction analysis showed that both ZnO nanostructures obtained by [10, 16] have a hexagonal wurtzite phase without any impurity observed. Several researches indicate the hexagonal wurtzite structure of ZnO nanomaterials. Sun et al. [15] deposited ZnO nanorods on Si substrate at 600°C, and the XRD analysis exhibits that well-aligned ZnO nanorods have a hexagonal wurtzite structure with high *c*-axis aligned. Lepot et al. [17] prepared ZnO nanorods at 80°C for 48 h. Also, they assigned a hexagonal wurtzite type as a crystal structure for the ZnO nanorods obtained, and no intermediate $Zn(OH)_2$ peaks were detected. That means the high purity and good crystallinity of the ZnO nanorods fabricated.

In this paper, porous layers of ZnO nanostructures like nanorods and nanoflowers were deposited on glass substrate and used as photocatalysts to remove the organic contaminants. The preparation of ZnO nanorods and nanoflowers over different seed layer positions was done by the hydrothermal method, and their photocatalyst application was studied. The crystalline structure of the ZnO nanostructures acquired was characterized, and the formation mechanism of ZnO nanoflowers was discussed. Furthermore, the photocatalytic achievements of ZnO nanorods and nanoflowers were tested, and the photodegradation of organic dye was investigated.

2. Experimental Procedure

2.1. Synthesis of ZnO Seeds. The seed layers were deposited on soda lime glass substrate by a Radiofrequency Sputtering (RFS) Nanovak NVTS 400 vacuum system. The ZnO thin films were prepared, as seed layers via RF sputtering, by means of a target of ZnO. The pressure, Argon gas flow, and the power as conditions of deposition were mentioned as 8 mToor, 40 W, and 5.5 sccm, respectively. At room temperature (27°C) and for 120 min, the soda lime glasses were coated with 200 nm thickness of ZnO thin films.

2.2. Growth of ZnO Nanostructures. In order to synthesize ZnO nanorods and nanoflowers, an aqueous solution was prepared with a 2.1 M of sodium hydroxide NaOH (99.99% Sigma-Aldrich) and 0.15 M of zinc nitrate $Zn(NO_3)$. $6H_2O$ (99.99% Sigma-Aldrich) were dissolved in deionized water (pH = 6.8). The growth solution was transformed to three Teflon Lined Sealed Stainless Steel Autoclaves, and the seeds deposited by RF sputtering were immersed in this solution with three different positions: slanted, surface up, and surface down. The ZnO nanostructures were grown over seeds in an oven at 120°C for 3 h as deposition time. After this process, the ZnO nanorods and nanoflowers obtained were removed from the solution after cooling, rinsed with deionized water, and dried in air at 60°C. The schema of the ZnO nanorod and nanoflower formation is illustrated in Figure 1.

2.3. Photocatalysis Process. To investigate the photocatalytic activity, of Methylene Blue ($C_{16}H_{18}C_lN_3S$) with a concentration of 2 mg/l, ZnO nanostructures were formed at various substrate surfaces through the hydrothermal method. The ZnO nanorods and nanoflowers prepared were dipped in the solution of MB and irradiated with UV light source of $\lambda = 254$ nm. To estimate the photocatalysis activities of ZnO nanostructures, ZnO nanorods/glasses and ZnO nanoflowers/glasses were immersed into 30 ml Methylene Blue (MB) aqueous solution. Then, 3 ml reaction samples were retired periodically for UV-vis analysis. The removal of MB dye was analyzed by following the absorbance variation of the peak at 664 nm after every 60 min for 300 min.

The as-product ZnO nanostructures were performed by an X-ray diffraction diffractometer. The chemical composition (EDS) and the surface morphology of these ZnO nanorods and nanoflowers were characterized via the energy-dispersive X-ray spectrometer and scanning electron microscopy (SEM). The optical properties and the photocatalytic measurement of ZnO nanostructures were analyzed by UV-visible spectroscopy.

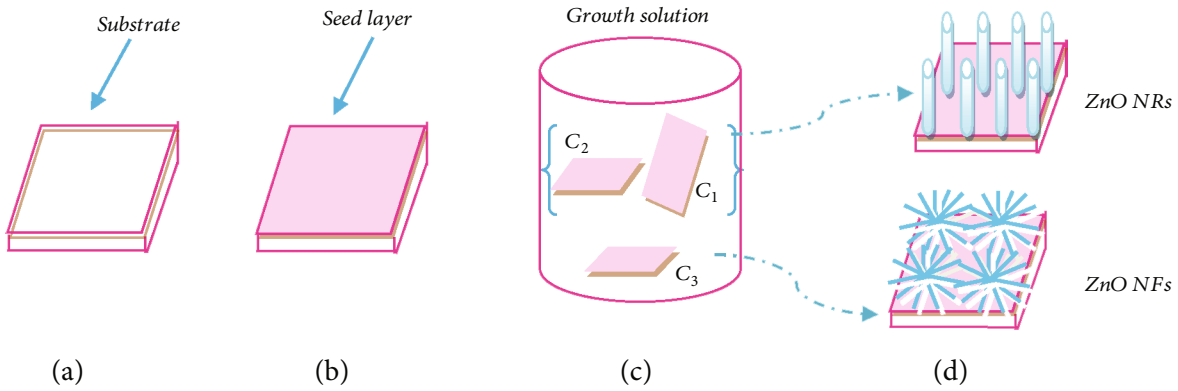

FIGURE 1: Schema of the ZnO nanorod and nanoflower formation: (a) soda lime glass substrate; (b) seed layer of ZnO by RF sputtering; (c) growth solution of NaOH and $Zn(NO_3)$. $6H_2O$ in Teflon Lined Sealed Stainless Steel Autoclaves with (C_1) substrate slanted, (C_2) surface down, and (C_3) surface up; (d) ZnO nanoflower and nanorod growth at 120°C for 3 h.

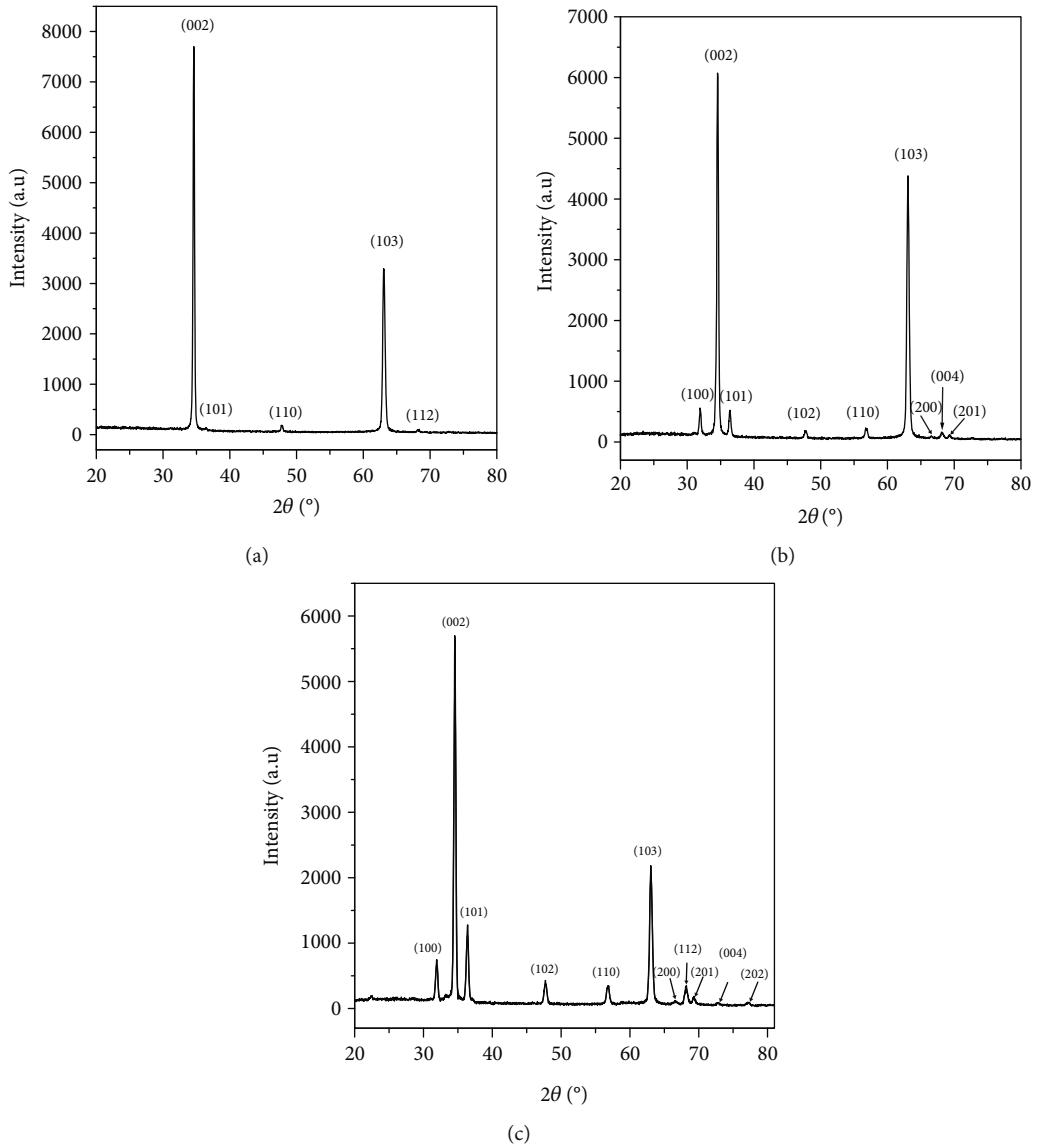

FIGURE 2: XRD pattern of ZnO nanostructures: (a) surface down nanorods, (b) surface up nanorods, and (c) surface slanted nanoflowers.

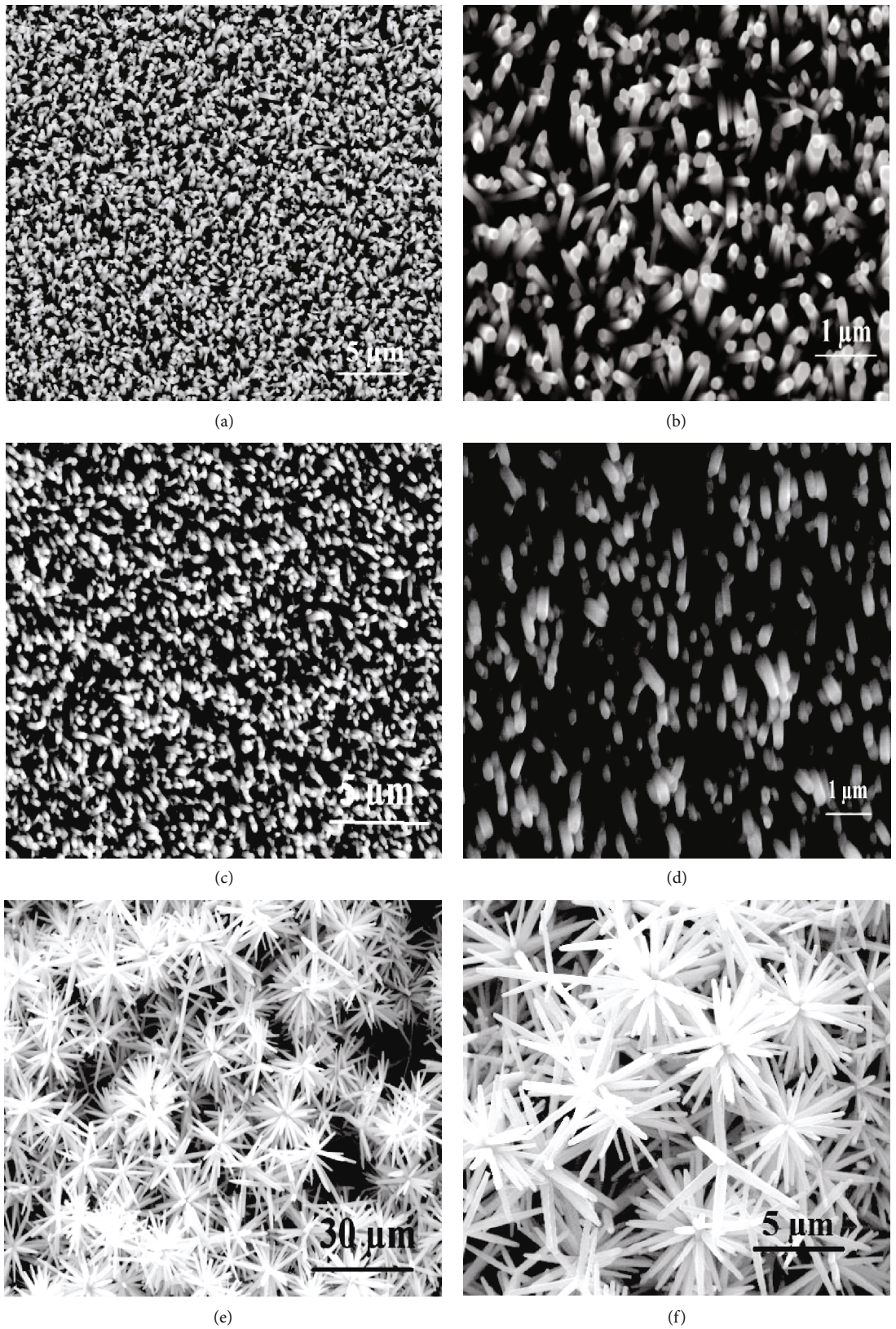

(a) (b) (c) (d) (e) (f)

Figure 3: SEM images of ZnO nanorods (a, b; c, d) and nanoflowers (e, f) at low and high magnifications.

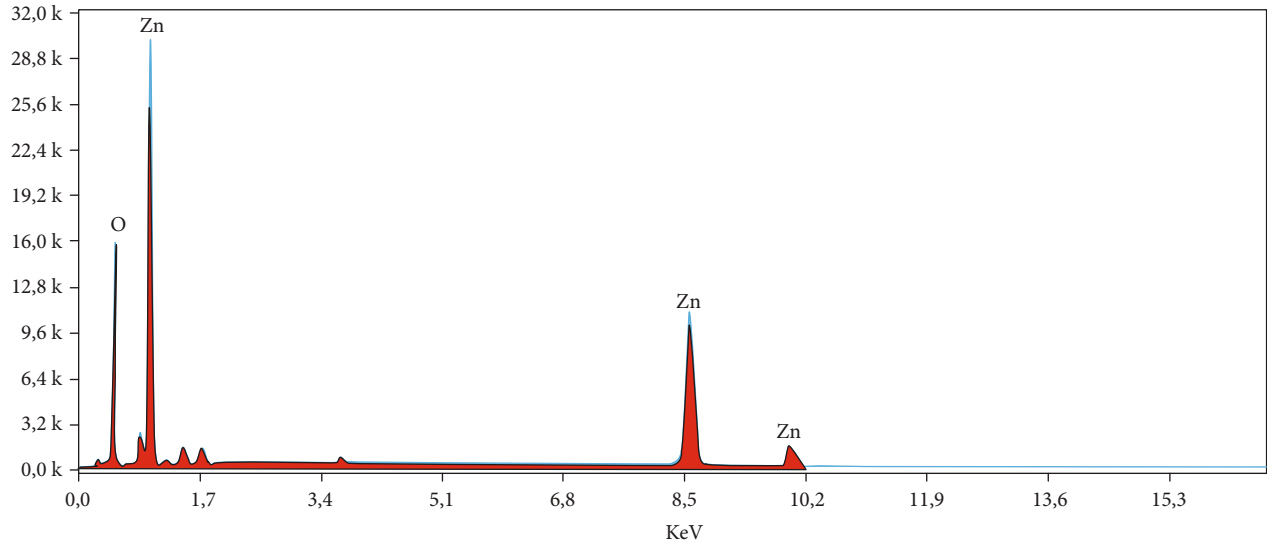

Figure 4: A typical EDS spectrum of ZnO nanoflowers.

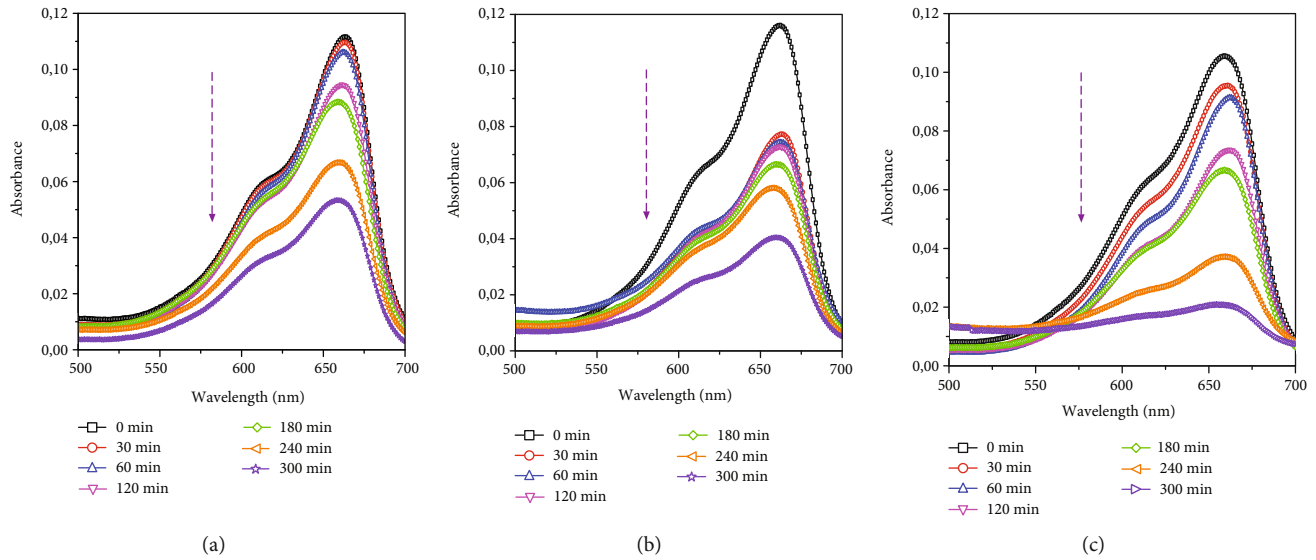

Figure 5: UV-vis absorption spectra of the degradation of MB dye solution in contact with ZnO: (a, b) nanorods; (c) nanoflowers.

3. Results and Discussion

Figure 2 shows the XRD pattern of ZnO nanorods (Figures 2(a) and 2(b)) and nanoflower (Figure 2(c)) synthesis via different seed layer substrate positions at 120°C for 3 h ((a) substrate surface up, (b) substrate surface down, and (c) substrate slanted). As can be seen, all diffracted peaks indexed the hexagonal wurtzite structure of ZnO with space group $P6_3mc$ and the lattice constants: $a = 0.3249$ nm, $c = 0.5206$ nm according to JCPDS: 36-1451. No additional peaks of $Zn(OH)_2$ were detected in the XRD pattern which means the formation of pure ZnO phase with high quality and impurity-free. The ZnO nanorods and nanoflowers show higher intensity of (002) peak which indicated that the preferential growth of rods and flowers is in the *c*-axis orientation [19]. As observed, in ZnO nanostructures synthesized with various substrate positions, there is an appearance of peaks such as (004) and (202) for ZnO nanoflowers (Figure 2(c)) and disappearance of peaks (100), (102), (200), (201), (004), and (202) for ZnO nanorods (Figure 2(a)). Moreover, a sharp, strong, and dominant peak at 34.59° confirms that the as-grown nanorods are single-crystalline with a wurtzite hexagonal phase and grown along the [0 0 0 1] direction. However, the well-aligned ZnO nanorods indicated that the rods are aligned vertically on substrate.

The surface morphology of ZnO nanostructures synthesized by the hydrothermal method with different substrate positions at 120°C and 3 h as a growth time was characterized by SEM and illustrated in Figure 3. Figures 3(a)–3(f) exhibit SEM images of ZnO nanorods and nanoflowers at low and high magnifications. As offered below in Figure 3, the surface substrate position has a great effect on the growth of ZnO nanostructures. Figures 3(a) and 3(b) exposed that the grown products are hexagonal nanorods and are vertically aligned

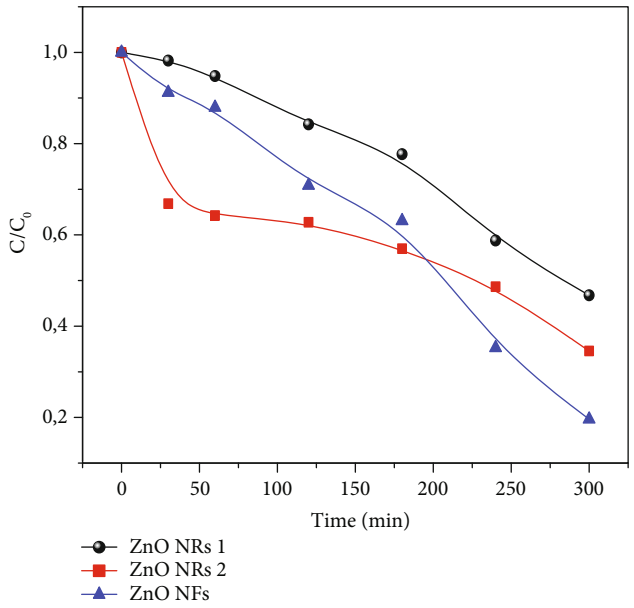

Figure 6: Photodegradation kinetic of MB dye by ZnO nanostructures.

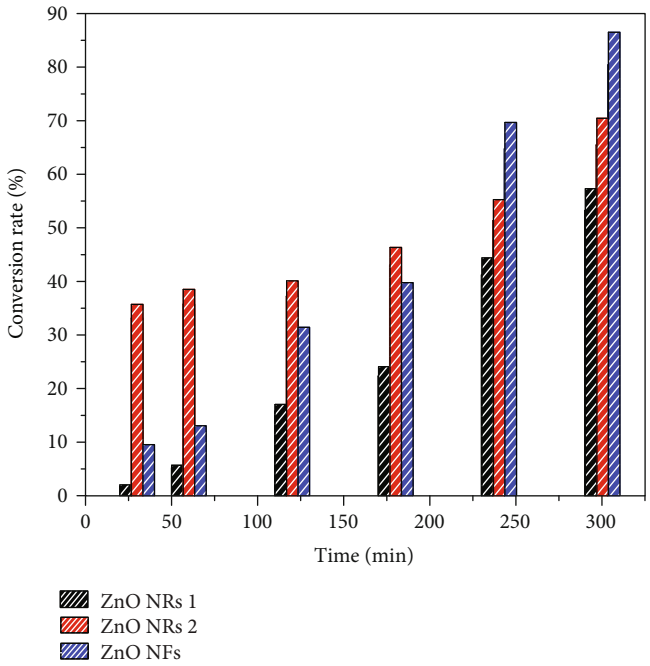

Figure 7: The photodegradation efficiency of MB dye by using ZnO nanorods and nanoflowers as photocatalysts.

to the substrate. It is very clearly seen from these images that the aligned hexagonal-shaped ZnO nanorods are grown onto the whole substrate surface in a high density.

The well-defined and perfect hexagonal faceted morphologies of the as-grown ZnO nanorods indicated that the synthesized products are single-crystalline with the wurtzite hexagonal phase (Figure 3(b)). The nanorods obtained (Figure 3(b)), with the surface down, have a hexagonal shape with different sizes of diameters which confirmed the XRD results. The measured diameters of the as-synthesized nanorods are ranged between 133.8 nm and 146.9 nm. Figures 3(c) and 3(d) indicated that ZnO nanorods were grown consequently of the slanted position of the seed layer substrate in low and high magnifications. As displayed, a high density of ZnO nanorods was formed on the full surface substrate as illustrated in Figure 3(c).

Figures 3(e) and 3(f) show that flower-like ZnO nanostructures were distributed on surface glass substrate for both magnifications low and high. From Figures 3(e) and 3(f), the growth of ZnO nanoflowers has a large-scale fabrication on the total surface of substrate. The process of growth of ZnO nanoflowers is concerning the precipitation of $Zn(OH)_2$ which is produced by the meeting of ions Zn^{2+} and OH^- in the solution. The formation of $Zn(OH)_4^{2-}$ ions has happened by successively dissolving $Zn(OH)_2$ in water. When the concentrations of $Zn(OH)_4^{2-}$ ions exceeded the critical value, ZnO nanoflowers were developed, and the relevant chemical reactions can be written as follows [20, 21]:

$$Zn^{2+} + 2\,OH \rightarrow Zn(OH)_2 \quad (1)$$

$$Zn(OH)_2 + 2\,OH^- \rightarrow Zn(OH)_4^{2-} \quad (2)$$

$$Zn(OH)_4^{2-} \rightarrow ZnO + HO + 2OH^- \quad (3)$$

Table 1: Reaction rate constant and photodegradation efficiency of various photocatalysts of ZnO.

ZnO nanostructures	Irradiation time (min)	Rate constant $K * 10^{-4}$ (min^{-1})	Photodegradation efficiency, η (%)
ZnO NRs 1	300	24.9	54
ZnO NRs 2	300	28.6	66
ZnO NFs	300	50.8	81

Figure 4 illustrated the typical EDS spectrum of ZnO nanoflowers which indicate that the synthesized products are composed of zinc and oxygen only. The EDS analysis affirms the formation of a pure ZnO phase which was in well agreement with the XRD results (Figure 2(c)).

The photocatalysis achievement was investigated by means of ZnO nanostructures for the applicability in photodegradation of organic dyes like Methylene Blue (MB). Figures 5(a)–5(c) show the photocatalytic performances of ZnO nanorods and nanoflowers. The variance of absorbance spectra of Methylene Blue solution under UV light irradiation with different ZnO nanostructures was carried out in the wavelength region between 500 nm and 700 nm. As mentioned, the absorption peak intensity is indicated as the signature of the dye degradation. As can be seen, the absorbance intensities decrease gradually with the increase of irradiation time from 0 to 300 min. Consequently, the photodegradation is very considerable when the solution of MB is in contact with ZnO nanoflowers then with ZnO nanorods that is indicating the successful reduction of ZnO nanoflowers.

For more understanding of photodegradation kinetics and the influence of seed layer position of ZnO nanostructures, we

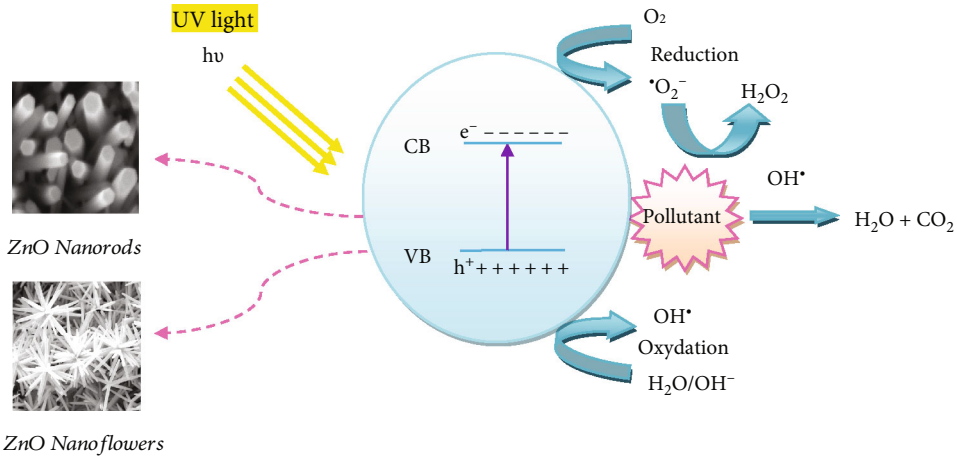

FIGURE 8: Schematic diagram describing the photocatalysis mechanisms of ZnO nanostructures.

have monitored the variation of the intensity of the absorption located at 664 nm. Figure 6 exhibits the variation of the ratio C/C_0 of the as-growth ZnO nanorods and nanoflowers, where C is the relative concentration at time t and C_0 is the initial relative concentration. As shown in Figure 6, the photodegradation kinetic of MB dye is reduced rapidly with increasing irradiation times for ZnO nanoflowers. However, the ratio is reduced slightly for both nanostructure samples: ZnO NRs 1 and 2. Furthermore, this ratio C/C_0 reaches 0.19, 0.34, and 0.44 after 300 minutes of irradiation for ZnO NFs and ZnO NRs 1 and 2, respectively.

The rate constant K was calculated by using the pseudo first-order kinetic law which can be defined as [22]

$$-\mathrm{Ln}\left(\frac{C}{C_0}\right) = kt. \tag{4}$$

The photocatalytic degradation efficiency of MB was computed by the following formula:

$$\eta\,(\%) = \frac{C_0 - C}{C_0}. \tag{5}$$

Figure 7 displays the photodegradation efficiency of Methylene Blue for all photocatalysts. The highest photocatalytic degradation efficiency was achieved at 81% by ZnO nanoflowers with the larger rate constant $K = 50.8 \times 10^{-4}$ min^{-1} for 300 min irradiation time. However, ZnO NRs 1 and ZnO NRs 2 as photocatalysts could degrade only 54% and 66% of MB during the same time of irradiation, respectively. The rate constant K for both nanostructures like rods was found 24.9×10^{-4} min^{-1} and 28.6×10^{-4} min^{-1} for ZnO NRs 1 and 2, respectively. As a result, ZnO nanoflowers are very suitable photocatalyst for organic dye photodegradation (MB). The efficiency and rate constant of each photocatalyst after 300 min of UV light exposure are given in Table 1.

The discrepancy in the photocatalytic activity of ZnO photocatalysts may found explication in the difference between their nanostructures. The porous structure, gap energy, lifetime of electron-hole pairs, and $^{\cdot}$OH radical concentration are fundamental parameters to ameliorate the efficiency of photocatalyst [23]. The migration of free charges to the surface of photocatalyst without recombining can participate in several oxidation and reduction reactions with adsorbed species such as oxygen, water, and other organic species by generating the hydroxyl radicals ($^{\cdot}$OH) which possess a high oxidation power. All reactions of the photocatalytic mechanism can be summarized by the following equations and Figure 8:

$$\mathrm{ZnO} + \mathrm{hv} \rightarrow \mathrm{e^-}_{\mathrm{CB}} + \mathrm{h^+}_{\mathrm{VB}} \tag{6}$$

$$\mathrm{e^-} + \mathrm{O_2} \rightarrow {}^{\cdot}\mathrm{O_2^-} \tag{7}$$

$$\mathrm{h^+} + \mathrm{OH^-} \rightarrow {}^{\cdot}\mathrm{OH} \tag{8}$$

$$\mathrm{h^+} + \mathrm{H_2O} \rightarrow \mathrm{H^+} + {}^{\cdot}\mathrm{OH} \tag{9}$$

$$^{\cdot}\mathrm{OH} + \mathrm{MB(dye)} \rightarrow \text{degradation products} \tag{10}$$

$$^{\cdot}\mathrm{O_2^-} + \mathrm{MB(dye)} \rightarrow \text{degradation products} \tag{11}$$

Generally, nanostructured films such as nanowires, nanobelts, and nanorods are recommended for humidity gas sensing, photocatalysis, and antibacterial activity due to the large specific surface [24–30] and to their high surface to volume ratio [31]. It has been demonstrated that photogenerated carrier recombination in ZnO, which is faster than the redox reactions involved in the photocatalysis process [32], hinders the photocatalytic activity [33]. Recently, material with a large surface to volume ratio such as nanostructured ZnO has achieved higher photocatalytic activity due to the large charge transfer in an open or porous structure [34, 35]. Thereafter, the enhancement in the photogenerated carriers from ZnO to liquid in a porous structure may explain the observed large photocatalytic efficiency in ZnO nanoflowers compared with ZnO nanorods.

4. Conclusion

ZnO nanorods and nanoflowers were successfully prepared by the hydrothermal method, and the enhancement in

photocatalysis efficiency of nanostructures was investigated. The XRD pattern exhibits that ZnO nanorods and nanoflowers have a wurtzite structure with the preferential growth of rods and flowers along the *c*-axis. The SEM images indicated the full growth of both nanostructures on glass substrate with high density. ZnO nanorod precipitations are well-aligned and have a hexagonal shape. The measured diameter of few hexagonal ZnO nanorods was found about 133.8 nm and 146.9 nm. The EDS analysis of ZnO nanoflowers shows the pure ZnO phase without any impurity. Moreover, the photodegradation efficiency of MB by ZnO nanostructures achieved 54%, 66%, and 81% for ZnO nanorods 1 and 2 and ZnO nanoflowers, respectively. The results obtained indicate that the surface position of seed layers can effectively modify the morphology of ZnO nanostructures, leading to the improvement of their photocatalytic performance. So, these ZnO nanoflowers are extremely significant for treatment of water.

Data Availability

No data were used to support this study.

Conflicts of Interest

The authors declare that they have no conflicts of interest.

References

[1] A. Mills and S. Le Hunte, "An overview of semiconductor photocatalysis," *Journal of Photochemistry and Photobiology A: Chemistry*, vol. 108, no. 1, pp. 1–35, 1997.

[2] T. K. Le, T. M. T. Nguyen, H. T. P. Nguyen et al., "Enhanced photocatalytic activity of ZnO nanoparticles by surface modification with KF using thermal shock method," *Arabian Journal of Chemistry*, 2017.

[3] I. Kazeminezhad and A. Sadollahkhani, "Influence of pH on the photocatalytic activity of ZnO nanoparticles," *Journal of Materials Science: Materials in Electronics*, vol. 27, no. 5, pp. 4206–4215, 2016.

[4] Z. R. Muslim, K. A. Aadim, R. F. Kadhim, and University of Baghdad, College of Science, Physics Department, "Preparation of ZnO for photocatalytic activity of methylene blue dye," *International Journal of Basic and Applied Science*, vol. 6, no. 1, pp. 1–7, 2017.

[5] Q. Zhou, B. Xie, L. Jin, W. Chen, and J. Li, "ydrothermal synthesis and responsive characteristics of hierarchical zinc oxide nanoflowers to sulfur dioxide," *Journal of Nanotechnology*, vol. 2016, Article ID 6742104, 6 pages, 2016.

[6] Y.-C. Yao, J.-M. Hwang, Z.-P. Yang et al., "Enhanced external quantum efficiency in GaN-based vertical-type light- emitting diodes by localized surface plasmons," *Scientific Reports*, vol. 6, no. 1, 2016.

[7] H. Shah, Manikandan, M. Basheer Ahmed, and V. Ganesan, "Enhanced bioactivity of Ag/ZnO nanorods-a comparative antibacterial study (Sbds)," *Journal of Nanomedicine & Nanotechnology*, vol. 04, no. 03, p. 168, 2017.

[8] R. Pietruszka, B. S. Witkowski, S. Gieraltowska et al., "New efficient solar cell structures based on zinc oxide nanorods," *Solar Energy Materials & Solar Cells*, vol. 143, pp. 99–104, 2015.

[9] W. Ludwig, W. Ohm, J.-M. Correa-Hoyos, Y. Zhao, M. C. Lux-Steiner, and S. Gledhill, "Electrodeposition parameters for ZnO nanorod arrays for photovoltaic applications," *Physica Status Solidi A: Applications and Materials Science*, vol. 210, no. 8, pp. 1557–1563, 2013.

[10] J. Fan, T. Li, and H. Heng, "Hydrothermal growth of ZnO nanoflowers and their photocatalyst application," *Bulletin of Materials Science*, vol. 39, no. 1, pp. 19–26, 2016.

[11] Y. Wang, X. Li, N. Wang, X. Quan, and Y. Chen, "Controllable synthesis of ZnO nanoflowers and their morphology-dependent photocatalytic activities," *Separation and Purification Technology*, vol. 62, no. 3, pp. 727–732, 2008.

[12] R. Mohan, K. Krishnamoorthy, and S. J. Kim, "Diameter dependent photocatalytic activity of ZnO nanowires grown by vapor transport technique," *Chemical Physics Letters*, vol. 539-540, pp. 83–88, 2012.

[13] L. N. Protasova, E. V. Rebrov, K. L. Choy et al., "ZnO based nanowires grown by chemical vapour deposition for selective hydrogenation of acetylene alcohols," *Catalysis Science and Technology*, vol. 1, no. 5, pp. 768–777, 2011.

[14] Y. Jouane, S. Colis, G. Schmerber et al., "Room temperature ZnO growth by rf magnetron sputtering on top of photoactive P3HT: PCBM for organic solar cells," *Materials Chemistry*, vol. 21, no. 6, pp. 1953–1958, 2011.

[15] Y. Sun, G. M. Fuge, and M. N. R. Ashfold, "Growth of aligned ZnO nanorod arrays by catalyst-free pulsed laser deposition methods," *Chemical Physics Letters*, vol. 396, no. 1-3, pp. 21–26, 2004.

[16] S. Kuriakose, N. Bhardwaj, J. Singh, B. Satpati, and S. Mohapatra, "Structural, optical and photocatalytic properties of flower-like ZnO nanostructures prepared by a facile wet chemical method," *Beilstein Journal of Nanotechnology*, vol. 4, pp. 763–770, 2013.

[17] N. Lepot, M. K. Van Bael, H. Van den Rul et al., "Synthesis of ZnO nanorods from aqueous solution," *Materials Letters*, vol. 61, no. 13, pp. 2624–2627, 2007.

[18] Y. Habba, M. Capochichi-Gnambodoe, and Y. Leprince-Wang, "Enhanced photocatalytic activity of iron-doped ZnO nanowires for water purification," *Applied Sciences*, vol. 7, no. 11, p. 1185, 2017.

[19] A. M. Peiró, P. Ravirajan, K. Govender et al., "Hybrid polymer/metal oxide solar cells based on ZnO columnar structures," *Materials Chemistry*, vol. 16, no. 21, pp. 2088–2096, 2006.

[20] Y. Sun, L. Wang, X. Yu, and K. Chen, "Facile synthesis of flower-like 3D ZnO superstructures via solution route," *CrystEngComm*, vol. 14, no. 9, p. 3199, 2012.

[21] P. Li, H. Liu, B. Lu, and Y. Wei, "Formation mechanism of 1D ZnO nanowhiskers in aqueous solution," *Journal of Physical Chemistry C*, vol. 114, no. 49, pp. 21132–21137, 2010.

[22] B. Li and Y. Wang, "Facile synthesis and photocatalytic activity of ZnO-CuO nanocomposite," *Superlattices and Microstructures*, vol. 47, no. 5, pp. 615–623, 2010.

[23] C. V. Reddy, B. Babu, and J. Shim, "Synthesis, optical properties and efficient photocatalytic activity of CdO/ZnO hybrid nanocomposite," *Journal of Physics and Chemistry of Solids*, vol. 112, pp. 20–28, 2018.

[24] Q. Wan, Q. H. Li, Y. J. Chen et al., "Positive temperature coefficient resistance and humidity sensing properties of Cd-doped ZnO nanowires," *Applied Physics Letters*, vol. 84, no. 16, pp. 3085–3087, 2004.

[25] S. P. Chang, S. J. Chang, C. Y. Lu et al., "A ZnO nanowire-based humidity sensor," *Superlattices and Microstructures*, vol. 47, no. 6, pp. 772–778, 2010.

[26] N. Zhang, K. Yu, Z. Zhu, and D. Jiang, "Synthesis and humidity sensing properties of feather-like ZnO nanostructures with macroscale in shape," *Sensors and Actuators A: Physical*, vol. 143, no. 2, pp. 245–250, 2008.

[27] X. Hu, J. Gong, L. Zhang, and J. C. Yu, "Continuous size tuning of monodisperse ZnO colloidal nanocrystal clusters by a microwave-polyol process and their application for humidity sensing," *Advanced Materials*, vol. 20, no. 24, pp. 4845–4850, 2008.

[28] Y. Qiu and S. Yang, "ZnO Nanotetrapods: controlled vapor-phase synthesis and application for humidity sensing," *Advanced Functional Materials*, vol. 17, no. 8, pp. 1345–1352, 2007.

[29] A. Erol, S. Okur, B. Comba, Ö. Mermer, and M. Ç. Arikan, "Humidity sensing properties of ZnO nanoparticles synthesized by sol-gel process," *Sensors and Actuators B: Chemical*, vol. 145, no. 1, pp. 174–180, 2010.

[30] W. Wang, Z. Li, L. Liu et al., "Humidity sensor based on LiCl-doped ZnO electrospun nanofibers," *Sensors and Actuators B: Chemical*, vol. 141, no. 2, pp. 404–409, 2009.

[31] L. Zhang, J. Zhao, H. Lu et al., "Facile synthesis and ultrahigh ethanol response of hierarchically porous ZnO nanosheets," *Sensors and Actuators B: Chemical*, vol. 161, no. 1, pp. 209–215, 2012.

[32] T. Xu, L. Zhang, H. Cheng, and Y. Zhu, "Significantly enhanced photocatalytic performance of ZnO via graphene hybridization and the mechanism study," *Applied Catalysis B: Environmental*, vol. 101, no. 3-4, pp. 382–387, 2011.

[33] B. Li and H. Cao, "ZnO@graphene composite with enhanced performance for the removal of dye from water," *Materials Chemistry*, vol. 21, no. 10, pp. 3346–3349, 2011.

[34] C. Zhang, L. Yin, L. Zhang, Y. Qi, and N. Lun, "Preparation and photocatalytic activity of hollow ZnO and ZnO-CuO composite spheres," *Materials Letters*, vol. 67, no. 1, pp. 303–307, 2012.

[35] A. Wei, L. Xiong, L. Sun, Y. J. Liu, and W. W. Li, "CuO nanoparticle modified ZnO nanorods with improved photocatalytic activity," *Chinese Physics Letters*, vol. 30, no. 4, pp. 046202–046205, 2013.